Pergamon

Int. J. Heat Mass Transfer. Vol. 37, No. 3, pp. 437–442, 1994

0017-9310/94 $6.00+0.00

An extended power law model for the calibration of hot-wire/hot-film constant temperature probes

S. WU

Institute for Marine Dynamics—National Research Council of Canada, P.O. Box 12093, Station A, St. John's, NF, A1B 3T5, Canada

and

N. BOSE

Naval Architectural Engineering, Faculty of Engineering and Applied Science, Memorial University of Newfoundland, St. John's, NF, A1B 3X5, Canada

(*Received* 13 *July* 1992 *and in final form* 22 *July* 1993)

Abstract—A systematic approach was taken towards deriving a unified and general model for the calibration of hot-wire/hot-film constant temperature probes. Considerations of the rate of heat transfer from these thermal sensors suggest this general calibration model in the form of an extended power law. This is preceded by a detailed review, and discussion regarding the validity and merits, of the various formulae that are in current use. An example is given of the calibration data obtained with a hot-film probe in a towing tank to compare the accuracy of these formulae. The results show much improved modelling accuracy with the current formulae.

INTRODUCTION

DESPITE advances made in the application of laser based measurement technology over the last two decades, constant temperature anemometry (CTA) is, apart from being cheap and simple, still a practical and very accurate tool for measurement of turbulence [1]. There are various formulae that are in use for the calibration of CTA operated hot-wire/hot-film probes. Among them, King's law [2] is well known. Others are either modified forms of King's law to suit specific cases, or expressions used for mathematical simplicity. There is a lack of a unified and general approach to modelling the calibration of hot-wire/hot-film probes. In the following, these formulae are reviewed and discussed. Attempts are then made to derive a more general calibration model by applying the laws of heat transfer to these thermal sensor probes. An example is given for comparative study to demonstrate the improved accuracy of the present model.

SUMMARY OF THE EXISTING MODELS

Table 1 gives a summary of the calibration models that are in common use. In the table, U is the calibration velocity (directed in the plane defined by the sensor and the probe axes, and normal to the sensor axis); V is the anemometer output voltage; A_k, $k = 0, 1, \ldots, m$, and n are experimental constants.

King's law [2] has long been used and was originally derived from the rate of forced heat convection from a long cylinder in a uniform flow, given as

$$H = c\,Nu\,\Delta T \tag{1}$$

where H is the rate of heat transfer; c is a coefficient; and ΔT is the temperature difference between the heat source (a heated sensor) and the cooling medium; and Nu is the dimensionless Nusselt number and is a function of the Reynolds number (defined in terms of the cylinder diameter), given, according to King [2], by

$$Nu = A'_0 + A'_1\,Re^{0.5}. \tag{2}$$

When applied to a cylindrical, constant temperature, thermal sensor, it becomes the well-known King's law. A'_k, $k = 0, 1$ are experimental constants.

However, King's law in equation (2) is inaccurate: when the Reynolds number is low, the effect of free convection (the buoyancy effect) becomes significant [10]; and when the Reynolds number varies over a wide range, the exponent takes different values over different Reynolds number ranges [11]. Other improved empirical forms have been suggested (e.g. [12–14]). These are complicated and this may have accounted for the lack in popularity for use with hot-wire/hot-film probe calibration. King's law is still commonly used for its simplicity. To achieve a better accuracy, *ad hoc* modifications have been made by freely varying the exponent, n (e.g. 3), or by adding a third term to King's law [4, 5]. Little consideration has been given to the theoretical justification. As free variation of n in the modified King's law form I (see Table 1) introduces nonlinearity, another simplification is often made by setting $A_0 = V_0^2$, where V_0 is the anemometer output voltage at zero velocity.

NOMENCLATURE

A_k	coefficients in the equations listed in Table 1, experimental constants	m	order of a polynomial
A'_k	coefficient of heat transfer, equations (2) and (3), experimental constants	Nu	Nusselt number
c	coefficient in equation (1)	n	exponent, an experimental constant
e_u, e_r and e_Σ	percentage curve fitting errors as defined in Tables 2, 3	Re	Reynolds number
H	forced heat convection rate	T	temperature
k	index of terms of a polynomial, $k = 0, 1, 2, \ldots, m$	ΔT	temperature difference between the sensor and the flow medium
		U	calibration velocity
		V	calibration voltage
		$\bar{V}$	curve fitted voltage
		V_0	calibration voltage at $U = 0$.

Table 1. List of commonly used calibration models for CTA operated hot-wire/hot-film probes

King's law [2]	$V^2 = A_0 + A_1 U^{0.5}$
Modified King's law I [3]	$V^2 = A_0 + A_1 U^n$
Modified King's law II [4]	$V^2 = A_0 + A_1 U^{0.5} + A_2 U$
Modified King's law III [5]	$V^2 = A_0 + A_1 U^{0.25} + A_2 U^{0.5}$
Polynomial U [6, 7]	$U = A_0 + A_1 V + A_2 V^2 + A_3 V^3 + \cdots + A_m V^m$
Polynomial V [8]	$V = A_0 + A_1 U + A_2 U^2 + A_3 U^3 + \cdots + A_m U^m$
Extended power law [9]	$V^2 = A_0 + A_1 U^n + A_2 U^{2n} + A_3 U^{3n} + \cdots + A_m U^{mn}$

Variation of V with U should then follow a linear relationship on a log–log (log $(V^2 - A_0)$ and log (U^n)) scale. The slope and the offset, which are equal to n and A_1 respectively, can then be found graphically or numerically from the plot (e.g. [15, 16]).

Bruun *et al.* [17] discussed these modified forms of King's law on the basis of simplicity and convenience for implementation on a micro or minicomputer. They suggested using a cubic spline fit to the smoothed raw calibration data. The form of a plain polynomial of V (denoted as polynomial V in Table 1 and below) was suggested to avoid the nonlinear complexity in the modified forms of King's law [8]. The form of a plain polynomial of U (referred to as polynomial U in Table 1) was suggested to achieve further simplicity from the viewpoint of voltage–velocity conversion [6,7]. These plain polynomial forms, although mathematically convenient, are unlikely to be more accurate, even with a polynomial of order of five, than King's law as they do not reflect the type of nonlinear relationship between the anemometer voltage and the calibration velocity. This nonlinear relationship results from Nu, which is directly proportional to the rate of heat transfer (i.e. power $\propto V^2$), being a function of Re to some power n, as empirical formulae suggest [11, 12].

A GENERAL CALIBRATION MODEL

A general calibration model can be obtained by choosing an appropriate form for $Nu = f(Re)$ that can represent this relationship more accurately and in a more general sense. In addition, this form must be mathematically convenient to use. Recognizing the nonlinear relationship between Nu and certain forms of Re^n, it is mathematically feasible to use a polynomial form of Nu in terms of Re^n. That is,

$$Nu = \sum_{k=0}^{m} A'_k \, Re^{kn} \tag{3}$$

which becomes the extended power law form shown in Table 1 when applied to the calibration of a constant temperature hot-wire/hot-film probe.

Compared with existing models, this extended power law has many advantages. Firstly, its use can be made simple mathematically: by downgrading its nonlinearity with a transformation of $y = V^2$ and $x = U^n$, it becomes a plain polynomial of y in terms of x. The experimental constants, A_k, and n can be determined by the conventional method of least squared regression; as n varies between 0 and 1, this is done by performing a least squares regression with a series of values of n that is varied from 0 to 1 successively. The set of values for A_k and n that corresponds to the minimum of the sum of the squared errors is taken as the solution [9].

Secondly, for the purpose of voltage-into-velocity conversion and probe angular sensitivity calibration, in which an explicit expression for U in terms of V, A_k, and n is preferred, this extended power law can be solved explicitly for U for $1 \leqslant m \leqslant 4$ [9]. With $m = 2$ and 3, for example, the extended power law can be rewritten as

$$U^n = \frac{-A_1 + \sqrt{(A_1^2 - 4A_2(A_0 - V^2))}}{2A_2} \quad (m = 2) \tag{4}$$

$$U^n = \sqrt[3]{(-q/2+r)} + \sqrt[3]{(-q/2-r)} - \frac{A_2}{3A_3} \quad (m = 3) \tag{5}$$

in which

$$r = \sqrt{\left(\left(\frac{q}{2}\right)^2 + \left(\frac{p}{3}\right)^3\right)};$$

$$p = \frac{3A_1A_3 - A_2^2}{3A_3^2};$$

and

$$q = \frac{3A_2^3 + 27A_3^2(A_0 - V^2) - 9A_1A_2A_3}{27A_3^3}.$$

Thirdly, equation (3) is more accurate in representing the heat transfer rate from these thermal sensors and the model might also allow partially for higher order effects, such as those due to free convection at low Reynolds numbers, and due to heat loss by conduction from the sensor to the sensor support. King's law and its modified forms shown in Table 1 are all specific cases of this extended power law.

EXPERIMENTAL RESULTS

Results were obtained from a towing tank calibration of a single sensor wedge-shaped hot-film probe (Dantec 55R32) with a DISA 55M01 anemometer. The probe was towed through still water in a towing tank by the towing tank carriage. The advantages of such calibration are twofold; the calibration velocity, which was equal to the carriage speed, can be measured very accurately (within 1 mm s^{-1} [18]); the still water in the tank has little turbulence. The maximum difference between two calibrations done over a two day period was under 1.7%. The present calibration was done at a steady tank water temperature in a time span of under one hour. The calibration techniques were similar to those used by Wu and Bose [19, 20].

DISCUSSION AND CONCLUSIONS

The curve fitting accuracy of the models in Table 1 to the calibration data is compared in Table 2. The percentage curve fitting errors in terms of voltage and measured velocity at individual calibration points are listed in Table 3. The following points can be made from the results.

(a) Plain polynomial V and U models did not give accurate fits to this data; even with a fifth order polynomial, the accuracy was barely of the same degree as modified King's law form I. These plain polynomials are also difficult to use for voltage–velocity conversion as the explicit form for U cannot be obtained with a fifth order polynomial.

(b) Modified King's law forms I and III did not lead to improved accuracy over King's law for this data. Modified King's law form II gave much improved accuracy over King's law. However, when these three models were applied to the calibration of a hot-wire probe in air [9], the modified King's law form II gave the least accurate result [9]. This indicates the *ad hoc* nature of these forms.

(c) The most significant improvement was obtained by using the extended power law form, even for a value of $m = 2$. Reduction in the total of squared errors was as much as 92% over use of King's law, and modified King's law forms I and III; and 58% over use of modified King's law form II. Still better results were achieved by using the extended power law with $m = 3$.

(d) The rate of improvement when m was increased from 2 to 3 was much less than when m was increased from 1 to 2 in the extended power law model. From a practical viewpoint, a value of $m \leqslant 3$ in this model is sufficient.

(e) Although the fitting accuracy of modified King's law form I seemed acceptable (under 1%), the resulting accuracy in the measured velocities was much lower. On the other hand, use of the extended power law model gave very accurate results over the whole velocity range (see Tables 2 and 3).

(f) A value of $A_0 < 0$ was obtained with the modified King's law form I. This indicates the inadequacy of King's law and modified King's law form I at low velocities. It was also found that with these two models, the maximum curve fitting error, which occurred at the low velocity end, increased as the calibration velocity range increased [9].

Problems with King's law and modified King's law form I for calibration at low velocities are further indicated in Figs. 1 and 2. In Fig. 1, the calibration results were plotted on a log $(V^2 - A_0)$ vs log U scale (i.e. $A_0 = V_0^2$). A chord line was also drawn between the two end points. The curve deviated from a straight line; this is similar to the results found by Davies [15, Fig. 4]. Errors will be introduced if a linear fit, as predicted by King's law and modified King's law form I, is used for this calibration. As a result, a velocity dependent value for n has been suggested by a number of researchers, e.g. [17]. Perry and Morrison [15] attributed one source causing the deviation of the calibration curve from a straight line (see Fig. 1) to the conventional static calibration technique. They suggested use of a dynamic calibration technique [15, 21]. However, the limitations of modified King's law form I itself can introduce large errors into the measurements. Results by Bruun [22] suggest that discrepancies found by Perry and Morrison [15], between the static and dynamic calibrations, were due to the inability of this modified King's law form I to accurately model the calibration curve over a wide calibration velocity range.

In Fig. 2, the same calibration results were plotted on a V^2 vs U^n scale. The point, $(U = 0, V_0)$, which

Table 2. Curve fitting results to the calibration data by using calibration models listed in Table 1; e_Σ is the sum of squared curve fitting errors, i.e. $e_\Sigma = \Sigma(V-\bar{V})^2$ with V and $\bar{V}$ being the calibration and curve fitted voltage, respectively

Mathematical model	Exponent n	A_0	A_1	A_2	A_3	A_4	A_5	$e_\Sigma \times 10^{-4}$
Polynomial V [6] ($m = 3$)		5.70	6.13	−3.83	0.89			726
Polynomial V [6] ($m = 4$)		5.45	8.21	−8.24	4.19	−0.80		196
Polynomial V [6] ($m = 5$)		5.26	10.36	−15.05	12.79	−5.45	0.90	52.5
King's law [2]	1/2	26.13	50.08					3597
Modified King's law I [3]	0.2280	−19.91	97.34					63.1
Modified King's law II [4]	1/2	13.40	83.94	−19.42				9.68
Modified King's law III [5]	1/4	−18.14	103.14	−7.50				62.1
Extended power law [9] ($m = 2$)	0.4598	9.96	87.06	−19.19				4.03
Extended power law [9] ($m = 3$)	0.5250	13.20	91.65	−31.80	4.77			3.57

Table 3. Percentage curve fitting errors at individual calibration points; e_U and e_V are the curve fitting errors in terms of voltage and measured velocity, respectively, defined as the absolute difference between calibration value and fitted value divided by calibration value

Calibration data		Modified King's law form I		Extended power law $m = 2$	
U (m s^{-1})	V (V)	e_V (%)	e_U (%)	e_V (%)	e_U (%)
0.091	6.608	0.41	2.36	0.01	0.05
0.192	6.826	0.33	2.02	0.09	0.54
0.293	7.290	0.50	3.15	0.12	0.77
0.396	7.656	0.22	1.44	0.00	0.01
0.496	7.929	0.13	0.87	0.06	0.36
0.596	8.170	0.11	0.77	0.07	0.43
0.697	8.367	0.20	1.35	0.06	0.38
0.797	8.530	0.16	1.11	0.04	0.29
0.949	8.764	0.35	2.45	0.10	0.67
1.100	8.942	0.24	1.73	0.01	0.05
1.302	9.152	0.17	1.20	0.02	0.17
1.503	9.325	0.03	0.21	0.05	0.38
1.756	9.508	0.20	1.44	0.07	0.61
2.009	9.677	0.31	2.20	0.08	0.66

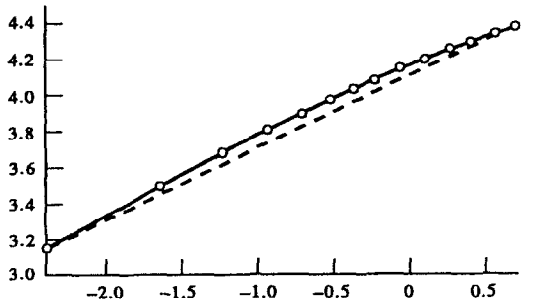

FIG. 1. A log–log plot of the calibration results. Coordinates: left ord: log $(V^2-V_0^2)$; abs: log (U). ○: calibration points; ———: a solid line drawn through the calibration points; - - - -: a chord line drawn between the two calibration points at the two ends.

was excluded when determining the experimental constants during the curve fitting, deviated substantially from that predicted by modified King's law form I. On the other hand, the extended power law with $m = 2$ or 3, modelled the nonlinearities at low velocities much more accurately. When the point, $(U = 0, V_0)$, was included when determining the experimental constants during the curve fitting (see Fig. 3), the curve fitting accuracy of the modified King's law form I was reduced markedly over the entire velocity range. Reduction in the curve fitting accuracy at high velocities was due to the inadequacy of this form to model the effect of free convection at low velocities. With the extended power law in both cases, the fitting was accurate over the entire velocity range.

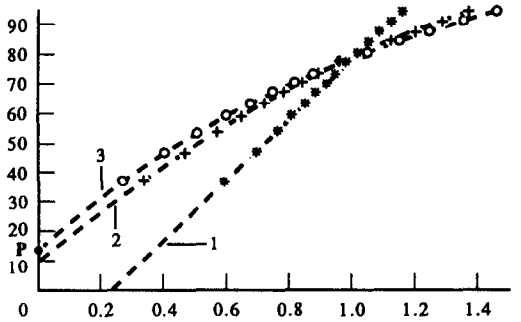

FIG. 2. A V^2 vs U^n plot of the calibration results and curve fits. **P** is the point ($U = 0$, V_0^2), and was excluded when determining the experimental constants during the curve fitting. The points marked with *, +, and ○ are the calibration data plotted for values of n (0.228, 4598, 0.525) appropriate for producing the best fit curves for the equations used; as the values of n change, the position of these points on this plot also changes. Coordinates: left ord: V^2; abs: U^n. * calibration data plotted with $n = 0.228$; + calibration data plotted with $n = 0.4598$; ○ calibration data plotted with $n = 0.525$; broken lines are curve fits: line 1—with modified King's law form I: $V^2 = -19.91 + 97.34U^{0.228}$; line 2—with extended power law ($m = 2$): $V^2 = 9.96 + 87.06U^{0.4598} - 19.19U^{2\times0.4598}$; line 3—with extended power law ($m = 3$): $V^2 = 13.2 + 91.65U^{0.525} - 31.8U^{2\times0.528} + 4.77U^{3\times0.525}$.

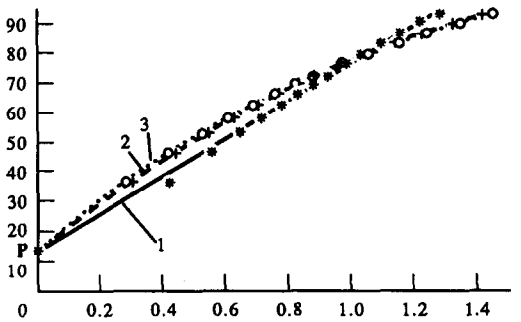

FIG. 3. A V^2 vs U^n plot of the calibration results and curve fits. In comparison with Fig. 2, the point **P** ($U = 0$, V_0^2) was included when determining the experimental constants during the curve fitting. The points marked with *, +, and ○ are the calibration data plotted for values of n (0.3766, 0.5018, 0.5317) appropriate for producing the best fit curve for the equations used. Coordinates: left ord: V^2; abs: U^n. The lines are the closest curve fits: line 1—with modified King's law form I: $V^2 = 13.44 + 63.37U^{0.3766}$; line 2—with extended power law ($m = 2$): $V^2 = 13.54 + 83.8U^{0.5018} - 19.43U^{2\times0.5018}$; line 3—with extended power law ($m = 3$): $V^2 = 13.54 + 91.9U^{0.5317} - 32.75U^{2\times0.5317} + 5.13U^{3\times0.5317}$.

(g) The significance of these improvements in curve fitting accuracy with the extended power law are also reflected in the results of the yaw sensitivity for the probe. Here, for a given yaw angle, the yaw function is defined as the ratio of the effective velocity over the calibration velocity [23]. The yaw angle is taken to be that between the calibration velocity vector and the sensor axis of the probe. Figure 4 shows the calculated

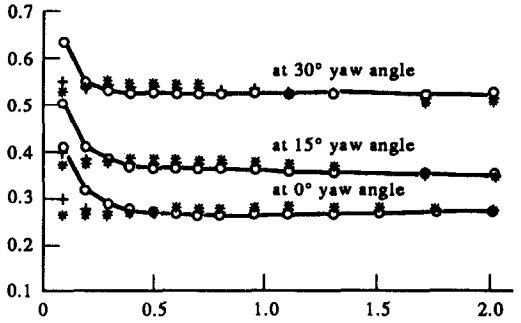

FIG. 4. Yaw function at three different yaw angles for one sensor of a dual sensor hot-film probe calculated with the modified King's law form I and the extended power law; the calibration data were from Wu and Bose [24]. Coordinates: left ord: yaw function; abs: calibration velocity (m s^{-1}). ○ calculated by using the modified King's law form I; + calculated by using the extended power law with $m = 2$; * calculated by using the extended power law with $m = 3$. The yaw function, at a given yaw angle, is defined as the ratio of the effective velocity [23] over the calibration velocity. A solid line is drawn to connect the points calculated by using the modified King's law form I.

results for the yaw function at three yaw angles for one sensor of a dual sensor hot-film probe [24]. The velocity dependence was significant when the modified King's law form I was used, but was reduced markedly when the extended power law was used with $m = 2$, and almost disappeared with $m = 3$.

(h) The above results show the importance of the value of n in all these models. It strongly depends on the value of m (see Table 2). Much has been discussed as to the appropriate value or values for n, e.g. [17], but with little agreement. Although fixed values for n are still used for reason of simplicity, among other considerations, it is generally accepted that a simultaneous solution for A_k and n leads to improved accuracy. However, the value for n in the extended power law may be purely the result of mathematical calculation. Experiments done with several probes under various conditions [20] showed that n varied from 0.19 up to 0.85.

Finally, use of the extended power law does not pose any more difficulty numerically than the other models in Table 1. Rather, because of the limited number of terms necessary in this extended power law model and because of the high accuracy that can be achieved, it might be considered a preferred model for the calibration of hot-wire/hot-film thermal sensor probes.

Acknowledgement—This work was part of a research project co-sponsored by the Canadian Centre for Fisheries Innovation, Newfoundland; Natural Sciences and Engineering Research Council of Canada; Avalon Propulsion Systems Ltd., St. John's, Newfoundland; the Institute for Marine Dynamics, National Research Council of Canada; and Seabright Corporation, St. John's, Newfoundland. We thank the Ocean Engineering Research Centre, Faculty of Engineering and Applied Science, Memorial University of Newfoundland, for use of the tank facilities.

REFERENCES

1. C. G. Lomas, *Fundamentals of Hot-Wire Anemometry*, Chap. 1. Cambridge Univ. Press, Cambridge (1986).
2. L. V. King, On the convection of heat from small cylinders in a stream of fluid: determination of the convection constants of small platinum wires, with applications to hot-wire anemometry, *Proc. R. Soc. London* **90,** 563–570 (1914).
3. A. G. Fabula, Operating characteristics of some hot film velocity sensors in water. In *Advances in Hot-Wire Anemometry, Proc. Int. Symp. Hot Wire Anemometry* (Edited by W. L. Melnik and J. R. Weske), pp. 167–193 (1967).
4. R. W. Siddall and T. W. Davies, An improved response equation for hot wire anemometry, *Int. J. Heat Mass Transfer* **15,** 367–368 (1972).
5. H. Win and J. M. Prahl, Calibration of constant-temperature hot-film anemometers at low velocities in water of uniform temperature, *Int. Commun. Heat Mass Transfer* **13,** 567–575 (1986).
6. W. K. George, P. D. Beuther and A. Shabbir, Polynomial calibrations for hot wires in thermally-varying flows. In *Symp. Thermal Anemometry* (Edited by D. E. Stock), ASME FED-Vol. 53, pp. 1–6 (1987).
7. Dantec Electronics, Inc., *'acqWire'—Technical Reference Manual*, a computer software developed by Dantec Electronics, Inc. (1990).
8. B. E. Thompson, Appraisal of a flying hot-wire anemometry, *Dantec Inf.*, no. 4, pp. 15–18 (1987).
9. S. Wu and N. Bose, Methods of fitting calibration curves to constant temperature anemometer data, Ocean Engineering Research Centre report: OERC91-WTT-TR003, Faculty of Engineering and Applied Science, Memorial University of Newfoundland (1991).
10. B. G. Van der Hegge Zijnen, Modified correlation formulae for heat transfers by natural and forced convection from horizontal cylinders, *Appl. Sci. Res.* **A6,** 129–140 (1956).
11. F. P. Incropera and D. P. DeWitt, *Fundamentals of Heat and Mass Transfer*, pp. 412–414. Wiley, New York (1990).
12. D. C. Collis and M. J. Williams, Two-dimensional convection from heated wires at low Reynolds numbers, *J. Fluid Mech.* **6,** 357–389 (1959).
13. A. Zhukauskas, Heat transfer from tubes in cross flow. In *Advances in Heat Transfer*, Vol. 8, pp. 93–160. Academic Press, New York (1972).
14. S. W. Churchill and M. Bernstein, A correlating equation for forced convection from gases and liquids to a circular cylinder in crossflow, *J. Heat Transfer* **99,** 300–306 (1977).
15. A. E. Perry and G. L. Morrison, Static and dynamic calibrations of constant-temperature hot-wire systems, *J. Fluid Mech.* **47,** 765–777 (1971).
16. DISA Elektroniks, Inc., *Instruction and Service Manual for Type 55D01 CTA*, DISA Elektronik A/S (1968).
17. H. H. Bruun, M. A. Khan, H. H. Al-Kayiem and A. A. Fardad, Velocity calibration relationships for hot-wire anemometry, *J. Phys. E: Sci. Instrum.* **21,** 225–232 (1988).
18. *Description of Tow Carriage C144, Operating Manual.* Kempf & Remmers GmbH, 2000 Hamburg, Germany (1983).
19. S. Wu and N. Bose, Axial wake survey behind a fishing vessel model by using a wedge-shaped hot-film probe, *J. Kansai Society of Naval Architects of Japan* **218,** 29–40 (1992).
20. S. Wu and N. Bose, Experience with hot-film probe for ship model nominal wake survey in a towing tank, *Proc. 23rd American Towing Tank Conference, New Orleans*, pp. 157–164 (June 1992).
21. P. J. Mulhearn and J. J. Finnigan, A simple device for dynamic testing of X-configuration hot-wire anemometer probes, *J. Phys. E: Sci. Instrum.* **11,** 679–681 (1978).
22. H. H. Bruun, A note on static and dynamic calibration of constant temperature hot-wire probes, *J. Fluid Mech.* **76,** 145–155 (1976).
23. F. E. Jorgensen, Directional sensitivity of wire and fibre-film probes, *DISA Inf.*, no. 11, pp. 31–37 (1971).
24. S. Wu and N. Bose, Methods of calibrating x-wire signals from constant temperature anemometers, Ocean Engineering Research Centre report: OERC91-WTT-TR005. Faculty of Engineering and Applied Science, Memorial University of Newfoundland (1991).